$PbTiO_3/SrTiO_3$ interface: Energy band alignment and its relation to the limits of Fermi level variation

Robert Schafranek,[1] Shunyi Li,[1] Feng Chen,[1] Wenbin Wu,[2] and Andreas Klein[1]
[1]*Technische Universität Darmstadt, Department of Materials and Earth Sciences, Surface Science Division, Petersenstraße 32, D-64287, Germany*
[2]*Hefei National Laboratory for Physical Science at the Microscale, University of Science and Technology of China, Hefei 230026, China*
(Received 15 April 2011; published 18 July 2011)

The interface formation between $PbTiO_3$ and $SrTiO_3$ has been studied by *in situ* photoelectron spectroscopy. A valence band offset of 1.1 ± 0.1 eV, corresponding to a conduction band offset of 1.3 ± 0.1 eV, is determined. These values are in good agreement with the band offsets estimated from measured ionization potentials of $SrTiO_3$ and $PbTiO_3$ surfaces. The observed band offsets are also in line with a $\sim$1.1 eV difference in barrier heights of $PbTiO_3$ in contact with different electrode materials as compared to barrier heights of $SrTiO_3$ with the same electrode materials. The results indicate that the band alignment is not strongly affected by Fermi level pinning and that the barrier heights are transitive. The limits of Fermi level variation observed from a number of thin films prepared on different substrates with different conditions are the same for both materials when these are aligned following the experimentally determined band offsets. By further comparing electrical conductivities reported for $SrTiO_3$ and $PbTiO_3$, it is suggested that the range of Fermi level position in the bulk of these materials, which corresponds to the range of observed conductivities, is comparable to the range of Fermi level position at interfaces with different contact materials. In particular the possibly low barrier height for electron injection into $SrTiO_3$ is consistent with the metallic conduction of donor doped or reduced $SrTiO_3$, while barrier heights $\gtrsim$1 eV for $PbTiO_3$ are consistent with the high resistivity even at high doping concentrations. The variation of barrier heights at interfaces therefore provides access to the range of possible Fermi level positions in the interior of any, including insulating, materials, which is relevant for understanding defect properties.

DOI: 10.1103/PhysRevB.84.045317 PACS number(s): 73.30.+y, 68.55.Ln, 77.84.−s, 79.60.Jv

I. INTRODUCTION

Ferroelectric and paraelectric perovskite thin films have been widely studied due to their various applications, e.g., as nonvolatile ferroelectric memories[1] or tunable capacitors for microwave devices.[2,3] Since more than a decade ago the scope has been extended to the research on perovskite oxide multilayers for the creation of materials with new properties not found in pure thin films. A wide variety of material combinations has been investigated including $SrTiO_3/BaTiO_3$,[4–7] $SrTiO_3/BaZrO_3$,[8] $PbTiO_3/PbZrO_3$,[9,10] $SrTiO_3/PbTiO_3$,[11–14] and others.[15] In the case of $SrTiO_3/PbTiO_3$ multilayers, a strong increase of ferroelectricity was observed for repetition units of $\{(SrTiO_3)_3/(PbTiO_3)_1\}$ and $\{(SrTiO_3)_3/(PbTiO_3)_2\}$,[12,13] which was attributed to *improper ferroelectricity*, originating from an interface effect.[13] The behavior of the multilayers is strongly different from those of the constituting materials in this case.

While the effect of stress on the dielectric and ferroelectric properties of these multilayer stacks was studied thoroughly,[4–6,9–14] the electronic interface properties are largely unresolved. One of the most important properties of semiconductor heterojunctions is the band alignment, meaning the discontinuities between valence and conduction bands at the interface. These determine, to a large extent, the potential distribution and the current transport through these interfaces.

$SrTiO_3$ (STO) and $PbTiO_3$ (PTO) are oxide semiconductors with similar band gaps of 3.2[16] and 3.4 eV,[1] respectively. The top of the $SrTiO_3$ valence band is derived mainly from O 2*p* states and the conduction band is largely derived from Ti 3*d* orbitals. In $PbTiO_3$ the Pb 6*s* states contribute significantly to both the valence and conduction band, which is due to Pb being present in a +II oxidation state in these compounds.[17,18] Another apparent difference between STO and PTO is their electrical conductivity behavior. While $SrTiO_3$ can be made highly *n*-type, e.g., by reduction or doping with Nb or La,[19] bulk $PbTiO_3$ is reported to be weakly *p*-type because of intrinsic doping by Pb vacancies.[20,21] The limits of electric conductivity are mainly caused by the limits of mobile carrier (electron and hole) concentrations. Since the concentrations of mobile carriers are defined by the energy distance between the Fermi level E_F and the band edges (E_{VB} and E_{CB}),[22] the range of accessible conductivities is directly related to the range of Fermi level positions. This phenomenon is known as self-compensation and related to the formation of compensating intrinsic defects, like oxygen or cation vacancies and interstitials.[23–26] Attempts have been made to generalize these doping limits for different materials by aligning these on a common energy scale.[24,26] The latter is best defined by the energy band alignment.

In this work we report on the determination of the energy band alignment between $SrTiO_3$ and $PbTiO_3$, as measured by *in situ* photoelectron spectroscopy during the interface formation. For the given combination, the energy band alignment estimated from electron affinity measurements, transitivity of barrier heights with various contact materials, and the direct determination of the band alignment are in good agreement with each other. A staggered band alignment, where the valence band of $PbTiO_3$ is $\sim$1.1 eV higher than the valence band of $SrTiO_3$, is observed. The energy band alignment further agrees with the range of Fermi level positions observed using photoemission from a number of thin films deposited

 ©2011 American Physical Society

Urheberrechtlich geschützt / In Copyright

with different conditions onto a range of substrates and also with the different electrical conductivities of the two materials.

II. BARRIER HEIGHTS OF $SrTiO_3$ AND $PbTiO_3$ INTERFACES

In this section a first derivation of the valence band offset ΔE_{VB} between $SrTiO_3$ and $PbTiO_3$ based on the transitivity rule is described. Transitivity is given when the band offsets between the materials A and B and materials B and C add up to the band offset of material A and C.[27] In case transitivity is fulfilled, which is often the case,[28] the difference of the Fermi energy position at the interface of $SrTiO_3$ and $PbTiO_3$ with various materials provides an estimate for the STO/PTO band alignment.

We have reported previously several *in situ* photoelectron spectroscopy interface studies of (Ba,Sr)TiO_3 (BST) and Pb(Zr,Ti)O_3 (PZT) with Pt,[29,30] RuO_2,[31–33] and In_2O_3:Sn (ITO),[32–34] respectively. The substitution with isovalent atoms does not typically lead to a strong shift of the band edge energies if the band gap is not affected. The latter is approximately true both for (Ba,Sr)TiO_3 and for Pb(Zr,Ti)O_3. It is therefore expected that barrier heights determined for BST are largely identical to those of STO and those determined for PZT should be comparable with those of PTO. The experimentally determined barrier heights are summarized in Fig. 1.

For the interface between Pt and (Ba,Sr)TiO_3 as well as between Pt and Pb(Zr,Ti)O_3, the Fermi energy position at the interface depends on the oxidation state of the interface.[29,30] Pt deposition leads to a reduction of the surface by formation of oxygen vacancies. These result in Fermi levels closer to the conduction band (see the dash-dotted lines in Fig. 1). After annealing in oxygen, the interfaces are oxidized accompanied by a reduction of defect concentration. The oxidation is accompanied by Fermi level shifts toward the valence band maximum. For the Pt interfaces, the Fermi level position in PTO lies 1.1 eV (0.9 eV) closer to the conduction band after Pt deposition (after annealing in oxygen) compared to STO. For the interfaces with RuO_2 and ITO, 1.1 eV and 1.3 eV lower Fermi level positions are observed in the case of $PbTiO_3$. The

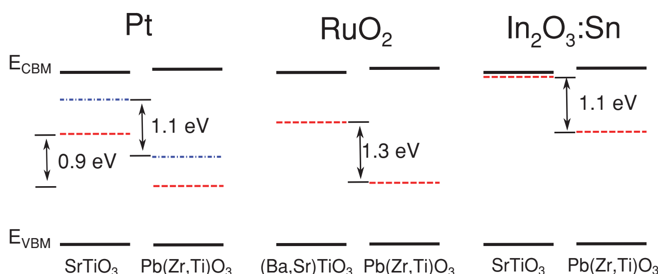

FIG. 1. (Color online) Fermi level positions at interfaces of (Ba,Sr)TiO_3 and Pb(Zr,Ti)O_3 with the electrode materials Pt, RuO_2, and In_2O_3:Sn, as reported in literature (Refs. 29–34). Depending on processing, there exist reduced (dash-dotted line) and oxidized (dashed line) states of the Pt interfaces with high and low Fermi level positions, respectively (Refs. 29 and 30). The distance between the interface Fermi level position in STO and PTO is shown for the different electrode materials. E_{CB} and E_{VB} are conduction band minimum and valence band maximum positions, respectively.

similar difference in Fermi level position at BST and PZT interfaces for three different contact materials indicates good transitivity and that the valence band maximum of $PbTiO_3$ is ~1.1 eV higher in energy compared with the valence band maximum of $SrTiO_3$.

III. ENERGY BAND ALIGNMENT AT $PbTiO_3/SrTiO_3$ INTERFACE

A. Experimental procedure

Photoemission experiments were performed at the DArmstadt Integrated SYstem for MATerial research (DAISY-MAT), which combines a Physical Electronics PHI 5700 multitechnique surface analysis system with several deposition chambers via an ultrahigh vacuum sample transfer.[35] X-ray photoelectron spectra were recorded using monochromatic Al Kα radiation with an overall energy resolution of ~0.4 eV, as determined from the Gaussian broadening of the Fermi edge of a sputter cleaned Ag sample. All XP spectra were taken using a takeoff angle of 45°. Ultraviolet induced photoelectron spectra were recorded in normal emission using He I radiation. All binding energies are given with respect to the Fermi level of a sputter cleaned Ag sample with an accuracy of ~50 meV.

The $PbTiO_3$ thin film used as substrate for the interface analysis was prepared by pulsed laser deposition using a KrF 248 nm excimer laser with a repetition rate of 10 Hz and an energy density of 1.8 J/cm^2. The PTO target was made by standard solid state reaction. The distance between the substrate and target during deposition was 5 cm, the substrate temperature 650 °C, and the oxygen pressure 30 Pa. Using these parameters, a growth rate of ~15 nm/min is obtained. A 50 nm thick PTO film was deposited on a 0.05 wt.% niobium-doped $SrTiO_3$(001) single crystal purchased from CrysTec. Epitaxial growth of PTO on STO is facilitated by the close lattice constants of $SrTiO_3$ and the *a*-lattice constant of tetragonal ferroelectric $PbTiO_3$ and has been achieved by several groups.[11,12] Epitaxial growth of our films has also been verified using x-ray diffraction.

For interface analysis, $SrTiO_3$ thin films were prepared in one of the deposition chambers of the DAISY-MAT system by radio frequency magnetron sputtering from a ceramic STO target. A power density of 1.25 W/cm^2, a substrate temperature of 500 °C, a pressure of 5 Pa, a substrate to target distance of 9 cm, and an Ar/O_2 ratio of 99/1 were used. The deposition rate for these conditions is 0.4 nm/min.

For surface cleaning of the *ex situ* prepared PTO, the thin film was heated for 30 min at 500 °C in 0.05 Pa O_2. As verified by XPS, this treatment leads to contamination-free surface, as also obtained for Pb(Zr,Ti)O_3 thin films.[30,32]

B. Surface potentials

A second value for the energy band alignment between STO and PTO can be obtained from the electron affinity rule (EAR),[36] which corresponds to an alignment of the vacuum level at the interface. It has to be mentioned, however, that due to the formation of interface dipoles, a considerable deviation of band alignment from the EAR estimate may occur.[37,38] In addition, the electron affinity of a material can considerably depend on the surface orientation and termination.[39–42] The

estimation of band alignment from electron affinities has therefore to be considered with great care.

$SrTiO_3$ surfaces have been widely studied using photoelectron spectroscopy.[43–46] Henrich *et al.* reported a work function of Ar-sputtered and vacuum annealed $SrTiO_3$ (001) single crystals of $\phi = 4.6$ eV and a distance between Fermi energy and valence band maximum $E_F - E_{VB} = 2.9$ eV after adsorption of oxygen to compensate for the oxygen loss during sputtering.[43] The ionization potential I_P, given by the energy difference between the vacuum energy and the valence band maximum, amounts to $I_P = \phi + E_F - E_{VB} = 7.5$ eV. This value agrees with the ionization potential measured at 0.05 wt.% Nb-doped $SrTiO_3$ (001) single crystals.[46] Taking the band gap E_g of $SrTiO_3$ of 3.2 eV into account,[16] an electron affinity $\chi = I_P - E_g = 4.3$ eV is obtained.

The ionization potential of the $PbTiO_3$ surface has not determined directly. Available values for surface potentials of Pb(Ti,Zr)O_3 surfaces are derived from (i) secondary electron emission of reduced bulk ceramic samples by Dixit *et al.*[47] and (ii) from XPS measurements across the interface of a PZT/Pt thin film sample by Scott *et al.*[48] The first work reports an ionization potential of 6.9 eV. Taking a band gap of PZT of 3.1 eV and assuming a mid-gap position of the Fermi energy a work function of 5.35 eV was deduced. In the other work an electron affinity of 3.5 eV for PZT, using the offset between the PZT and Pt spectra across the interface boundary, is derived. Finally a PZT work function of 5.8 eV and an electron affinity of 6.9 eV (identical to the one reported by Dixit *et al.*) were given by Scott *et al.*[48]

In Fig. 2 the UP spectra of the cleaned PTO thin film is shown. From the valence band spectrum a work function of 4.3 ± 0.05 eV can be deduced from the position of the secondary electron cutoff. The distance between Fermi energy and valence band maximum $E_F - E_{VB}$, as deduced from the linear extrapolation of the leading edge of the valence band spectrum, amounts to 1.9 ± 0.05 eV. Adding both values results in an ionization potential of 6.2 ± 0.1 eV and, with an energy gap of $PbTiO_3$ of 3.4 eV,[1] an electron affinity of 2.8 ± 0.1 eV is derived. To verify whether the UP spectra are incriminated by sample charging[32] it is useful to compare the $E_F - E_{VB}$ from XPS and UPS, since sample charging is typically more pronounced for UPS. As shown in the inset in Fig. 4, $E_F - E_{VB} = 1.85 \pm 0.05$ eV is measured via XPS, in good agreement with values derived from UPS. Sample charging is therefore excluded. The absence of charging in the XP and UP spectra of PTO is attributed to the low $PbTiO_3$ layer thickness. In any case, the ionization potential, which is used for deriving the band alignment rather than the work function, is not affected by charging effects.

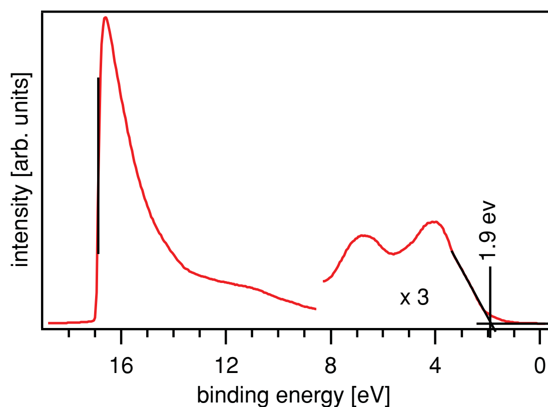

FIG. 2. (Color online) UP spectrum of the $PbTiO_3$ surface. The valence band maximum and the secondary electron edge positions are marked.

Following the electron affinity rule,[36] the STO/PTO band offsets can be estimated from the surface potentials of the respective perovskite materials. The valence band offset ΔE_{VB} and conduction band offset ΔE_{CB} are calculated from the difference in ionization potential $\Delta E_{VB} = I_p(\text{STO}) - I_p(\text{PTO})$ and difference in electron affinities $\Delta E_{CB} = \chi(\text{STO}) - \chi(\text{PTO})$, respectively. We find $\Delta E_{VB} = 1.3 \pm 0.2$ eV and $\Delta E_{CB} = 1.5 \pm 0.2$ eV. Within the experimental uncertainty the energy band alignment derived from the surface potentials agrees with the one derived from transitivity of barrier heights.

C. $PbTiO_3/SrTiO_3$ interface formation

X-ray induced photoelectron core level spectra of the $PbTiO_3$ thin film recorded in the course of $SrTiO_3$ deposition are shown in Fig. 3. During the stepwise deposition of $SrTiO_3$ the Pb cation intensity decreases and the Sr emission increases until a $SrTiO_3$ thickness of $\sim$8 nm is reached and the Pb emission is almost completely attenuated. The Pb substrate cation emission decays exponentially, indicating a layer-by-layer growth mode. The Pb emission line shape does not change with increasing STO layer thickness. Furthermore the Ti 2*p* and O 1*s* line shapes do not change with increasing STO thickness, although the signal originates increasingly from the $SrTiO_3$ overlayer. The rising background at higher binding energies and low STO coverage in the Sr 3*d* spectrum is an extension of the Pb 4*f* emission at $\sim$138 eV and incriminate neither the binding energy position nor the line shape of the Sr 3*d* doublet. Hence, from the constant line shapes of all substrate and deposit lines, an abrupt interface formation is indicated.

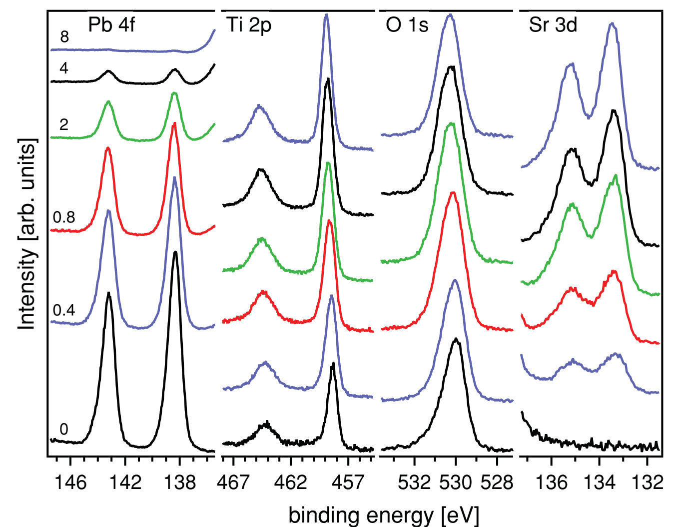

FIG. 3. (Color online) X-ray photoelectron core level spectra of the $PbTiO_3$ sample recorded in the course of $SrTiO_3$ deposition. The STO thickness is given in nm.

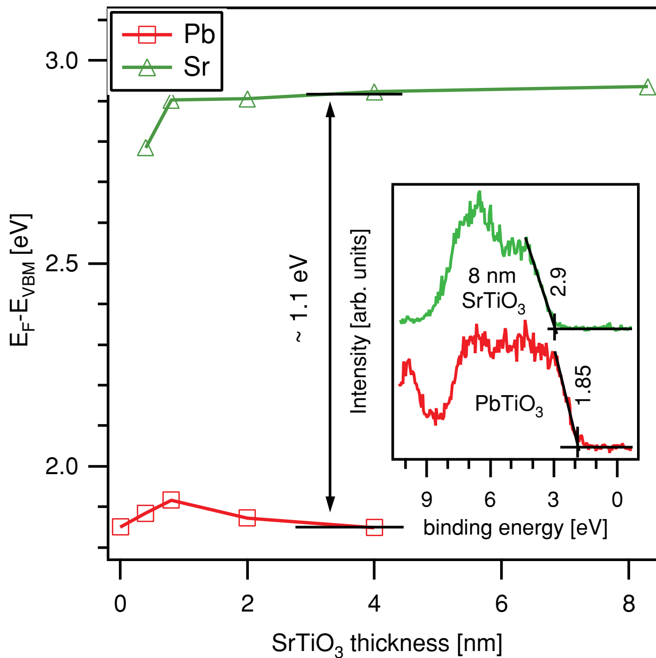

FIG. 4. (Color online) The binding energy of the Pb $4f_{7/2}$ and Sr $3d_{5/2}$ emission lines with respect to the corresponding valence band maximum position are shown in dependence on the $SrTiO_3$ film thickness. The insert features XP valence band spectra of the uncovered PTO sample and of the 8 nm thick STO film.

The evolution of the binding energies of the Pb and Sr emission lines are shown in Fig. 4 in the course of $SrTiO_3$ deposition. Binding energies of the core levels are referenced to the binding energy of the valence band maxima of the uncovered $PbTiO_3$ substrate and of the 8 nm thick $SrTiO_3$ film for better comparison. The binding energy differences between core levels and valence band maxima are within ± 0.1 eV of the average values of a large set of comparable samples.

The XPS valence band spectra for the PTO substrate and the STO film are presented in the inset of Fig. 4. Valence band maxima positions of 1.85 ± 0.05 eV and 2.95 ± 0.05 eV are derived for $PbTiO_3$ and $SrTiO_3$, respectively. The binding energy of the Pb 4*f* emission, representing the valence band maximum of the PTO substrate, increases slightly after deposition 0.4 and 0.8 nm STO and returns to the original value of the uncovered PTO after 4 nm STO deposition. The Sr 3*d* emission, representing the valence band maximum of the growing STO film, exhibits only small binding energy shifts with increasing film thickness. These shifts are not in parallel to those of the Pb 4*f* emission as would be expected for changes of the Fermi level position at the interface. However, the evolution of the electronic structure of the $SrTiO_3$ film with film thickness can also contribute to the shifts of the Sr 3*d* level. It is therefore most reasonable to determine the valence band offset at maximum $SrTiO_3$ thickness where the Pb 4*f* signal is still clearly detected. At 4 nm film thickness, the difference between the PTO and the STO valence band maxima amounts to $\Delta E_{VB} = 1.1 \pm 0.1$ eV with the valence band maximum of $SrTiO_3$ below that of $PbTiO_3$. Using the energy gaps of 3.2 eV for STO and 3.4 eV for PTO this corresponds to a conduction band offset of $\Delta E_{CB} = 1.3 \pm 0.1$ eV. The energy band alignment is in good agreement with those estimated from transitivity of barrier heights (see Sec. II) and from the ionization potentials (see Sec. III B).

IV. DISCUSSION

The different experimental approaches applied to determine the energy band alignment between two high-permittivity oxides, $SrTiO_3$ and $PbTiO_3$, are in very good agreement with each other. The directly determined value for the valence band discontinuity at the $SrTiO_3/PbTiO_3$ interface is $\Delta E_{VB} = 1.1 \pm 0.1$ eV, with the valence band maximum of $SrTiO_3$ below that of $PbTiO_3$. This is a reasonable result in the light of the different electronic structure of the materials. While the valence bands in STO are largely formed by the oxygen *p* states, there is an additional contribution of Pb 6*s* electrons to the valence bands in PTO, as Pb occupies the A site in the perovskite lattice and is therefore present in a +II oxidation state leaving the Pb 6*s* orbitals occupied. Electronic structure calculations reveal that the Pb 6*s* orbitals contribute significantly to the topmost valence states.[17,18] It can therefore be assumed that the valence band maximum of PTO is higher than that of STO, in good agreement with the experiments. The experimentally derived valence band offset therefore suggests that the band alignment is roughly given by alignment of the O 2*p* derived valence states. This common-anion-like alignment is in good agreement with the very small valence band discontinuities observed at interfaces between a series of oxides including (Ba,Sr)TiO_3, In_2O_3, ZnO, SnO_2 and Al_3O_3,[34,49–51] and with the small valence band discontinuities of common anion chalcogenides, which also have considerable ionic bonds.[52,53] An upward shift of the valence band maximum when cation *s* or *d* states contribute to the valence band density of states is also known for other compounds.[54,55]

It has been suggested in the literature that the barrier heights depend significantly on the ferroelectric polarization state.[56,57] The derived band alignment would then be affected by such polarization dependence. It is noted, however, that recent photoemission experiments at interfaces of a polycrystalline PZT ceramic, which exhibits multiple polarization and grain orientation, have revealed a single barrier height for the whole surface.[33] This indicates that the barrier heights might not depend on polarization. However, additional experiments would be required to settle this issue.

The directly determined valence band offset agrees with the difference in ionization potential. The energy band alignment is therefore not expected to be significantly influenced by Fermi level pinning caused by induced gap states. A corresponding calculation suggests a rather strong Fermi level pinning and a valence band offset of $\Delta E_{VB} = 0.7$ eV,[17] which is significantly smaller than the value derived from the present experiments. Absence of strong Fermi level pinning at interfaces of STO and PTO is also indicated by the large difference in barrier heights in dependence on contact material if nonreactive contact materials are employed.[32]

The experimentally deduced band alignment coincides very well with the observed ~1.1 eV lower Fermi level position at interfaces of PTO with different contact materials as compared to interfaces of STO. This holds for the interfaces with Pt,

RuO_2, and ITO and shows that the band alignments at the interfaces are transitive.

Most interestingly, the relative position of the band edges derived from the band alignment also seems to represent the differences in electronic transport properties of the two model perovskite materials $SrTiO_3$ and $PbTiO_3$. Wide band gap materials like STO and PTO can often not be highly doped *n*-or *p*-type, which is related to creation of self-compensating intrinsic points defects.[23,25] The doping limits of materials, but also the defect levels of transition-metal or hydrogen impurities, have been related to the absolute position of the band edges.[24,26,58–61] $SrTiO_3$ and $BaTiO_3$ exhibit an asymmetric dopability where donor doping (e.g., by La or Nb) or reduction can induce high electron conductivity.[19,62–64] In contrast, only weak *p*-type conductivity is observed for acceptor (e.g., Fe) doped $SrTiO_3$ at high temperatures and high oxygen pressures.[65] This doping asymmetry with a clear preference for *n*-type conductivity, i.e., for Fermi level positions closer to the conduction band, is also reflected in the barrier heights determined at interfaces of $SrTiO_3$ with different contact materials. The Fermi level positions at the different interfaces is reproducibly found in the upper half of the energy gap (see Fig. 1).

In contrast to $(Ba,Sr)TiO_3$, no high room temperature electrical conductivity has been reported for donor and acceptor doped $PbTiO_3$ or PZT. The absence of strong electrical conductivity corresponds to low concentrations of electrons and holes and hence to bulk Fermi level positions far apart from the valence and conduction band. This is also in good agreement with the determined barrier heights at the interfaces, which reveal interface Fermi level positions $\geqslant 1$ eV away from the band edges. The Fermi level at the PTO and PZT interfaces never comes close to valence or the conduction band. According to the interface experiments, the smallest barrier height for hole injection ($E_F - E_{VB}$) is smaller than the smallest barrier height for electron injection ($E_{CB} - E_F$). This is in agreement with fairly weak *p*-type conductivity of $PbTiO_3$ discussed in literature.[20,66]

This leads to the suggestion that the ranges of Fermi level positions observed at interfaces of BST and PZT with different contact materials are closely related to the range of Fermi level positions in the bulk of these two materials. Additional strong evidence for such a relation comes from the Fermi level positions ($E_F - E_{VB}$) measured at surfaces of BST and PZT samples. All measured films from which reliable binding energies can be determined show $E_F - E_{VB}$ values within the range covered by the data shown in Fig. 5, which include values from $(Ba,Sr)TiO_3$ and $Pb(Zr,Ti)O_3$ thin films with different Ba/Sr and Zr/Ti ratios. When the energy bands of BST are PZT are aligned according to the offset derived above as done in Fig. 5, the ranges of $E_F - E_{VB}$ at the surfaces of the two materials are in excellent agreement with each other and with the range of Fermi level positions measured at the different interfaces (see Fig. 1). The overall variation of Fermi level position in BST and PZT is of the same magnitude and amounts to < 1.5 eV, which is in excellent agreement with the allowed variation obtained from defect calculations (see Fig. 2 in Ref. 63). A very similar variation of the Fermi level is also observed for Sn-doped In_2O_3 and Al-doped ZnO.[41,51,67]

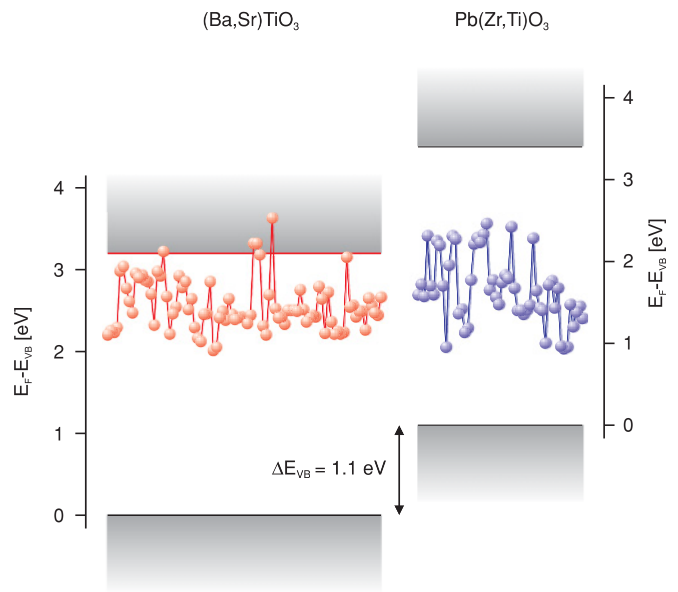

FIG. 5. (Color online) Fermi level positions at the surfaces of $(Ba,Sr)TiO_3$ and $Pb(Ti,Zr)O_3$ surfaces measured using photoelectron spectroscopy. The energy bands of $Pb(Ti,Zr)O_3$ and $(Ba,Sr)TiO_3$ are aligned according to the experimentally determined band offset of $\Delta E_{VB} = 1.1$ eV. The observed variation of Fermi level at the surfaces agrees with the range of Fermi level positions at interfaces with different materials (see Fig. 1). It also reflects the achievable doping in the two materials.

As the Fermi level position in the bulk of a material is impossible to access if no electrical transport measurements are possible, as is the case for insulating materials, the close correspondence between bulk, surface, and interface Fermi levels offers a strategy to overcome this limitation. The knowledge of Fermi level positions is particularly relevant for the defect properties of a material, as formation energies of charged defects directly depend on Fermi level position.

V. SUMMARY AND CONCLUSION

The band alignment between $PbTiO_3$ and $SrTiO_3$, a material system which exhibits considerably different properties in multilayer form (e.g., as a heterojunction) as compared to the pure materials, has been determined. The experiments were carried out using *in situ* photoelectron spectroscopy during the interface formation. A $PbTiO_3$ thin film grown epitaxially by pulsed laser deposition onto a $SrTiO_3$:Nb (001) single crystal was used as substrate material. The subsequent deposition of $SrTiO_3$ was performed *in situ* via rf magnetron sputtering. A valence band offset of 1.1 ± 0.1 eV, corresponding to a conduction band offset of 1.3 ± 0.1 eV, is determined, with the PTO band edges higher than the STO band edges. The energy band alignment is in good agreement with the difference in ionization potential, which is determined as 6.2 eV for PTO and 7.5 eV for STO, indicating absence of strong Fermi level pinning. The staggered energy band alignment is described by a common-anion-like alignment of the O 2*p* derived valence bands of both materials. The higher valence band maximum

of PTO can be rationalized by the contribution of the Pb 6*s* electrons to the topmost electronic states in the PTO valence band. The $PbTiO_3/SrTiO_3$ energy band alignment is further in agreement with the difference in barrier heights at interfaces of PZT and BST with different contact materials. This indicates that transitivity of band lineups is fulfilled for this system.

The range of Fermi level positions at different interfaces of STO (BST) and PTO (PZT) corresponds with the range of observed Fermi level positions at surfaces of these materials and with the ranges of Fermi level positions in the bulk, which is anticipated from the electrical conductivity of the doped materials. This underlines that the variation of Fermi level position is comparable in the bulk, at the surface, and at interfaces. The observed range of Fermi level positions, which is defined by the intrinsic defect properties of materials, illustrates nicely that $SrTiO_3$ can be highly doped while $PbTiO_3$ remains an insulator even at high doping levels. This observation also suggests that the determination of Fermi level positions at surfaces and interfaces using photoelectron spectroscopy can provide experimental access to the range of Fermi level positions in the bulk and thereby the dopability of any material. The limitation of low conductivity may be overcome by the investigation of thin films on electrically conducting substrates or the deposition of ultrathin electrically conduction contact materials on top of a thick insulator. Both sample structures provide the Fermi level reference required for an absolute measurement of $E_F - E_{VB}$. Such measurements can contribute to the understanding of doping limits and defect properties.

ACKNOWLEDGMENTS

This work was supported by the German Science Foundation (DFG) within the collaborative research center SFB 595 (Electrical Fatigue of Functional Materials).

[1]J. F. Scott, *Ferroelectric Memories* (Springer Verlag, Heidelberg, 2000).
[2]A. K. Tagantsev, V. O. Sherman, K. F. Astafiev, J. Venkatesh, and N. Setter, J. Electroceram. **11**, 5 (2003).
[3]S. Gevorgian, IEEE Microwave Mag. **10**, 93 (2009).
[4]H. Tabata, H. Tanaka, and T. Kawai, Appl. Phys. Lett. **65**, 1970 (1994).
[5]B. D. Qu, M. Evstigneev, D. J. Johnson, and R. H. Prince, Appl. Phys. Lett. **72**, 1394 (1998).
[6]J. Kim, Y. Kim, Y. S. Kim, J. Lee, L. Kim, and D. Jung, Appl. Phys. Lett. **80**, 3581 (2002).
[7]J. M. Zhang, A. Visinoiu, F. Heyroth, F. Syrowatka, M. Alexe, D. Hesse, and H. S. Leipner, Phys. Rev. B **71**, 064108 (2005).
[8]H. M. Christen, E. D. Specht, S. S. Silliman, and K. S. Harshavardhan, Phys. Rev. B **68**, 020101 (2003).
[9]I. Kanno, S. Hayashi, R. Takayama, and T. Hirao, Appl. Phys. Lett. **68**, 328 (1996).
[10]T. Choi and J. Lee, Thin Solid Films **475**, 283 (2005).
[11]J. C. Jiang, X. Q. Pan, W. Tian, C. D. Theis, and D. G. Schlom, Appl. Phys. Lett. **74**, 2851 (1999).
[12]M. Dawber, C. Lichtensteiger, M. Cantoni, M. Veithen, P. Ghosez, K. Johnston, K. M. Rabe, and J. M. Triscone, Phys. Rev. Lett. **95**, 177601 (2005).
[13]E. Bousquet, M. Dawber, N. Stucki, C. Lichtensteiger, P. Hermet, S. Gariglio, J.-M. Triscone, and P. Ghosez, Nature (London) **452**, 732 (2008).
[14]A. T. J. van Helvoort, O. Dahl, B. G. Soleim, R. Holmestad, and T. Tybell, Appl. Phys. Lett. **86**, 092907 (2005).
[15]H. N. Lee, H. M. Christen, M. F. Chisholm, C. M. Rouleau, and D. H. Lowndes, Nature (London) **433**, 395 (2005).
[16]M. Cardona, Phys. Rev. **140**, A651 (1965).
[17]J. Robertson, J. Vac. Sci. Technol. B **18**, 1785 (2000).
[18]S. Piskunov, E. Heifets, R. I. Eglitis, and G. Borstel, Comput. Mater. Sci. **29**, 165 (2004).
[19]O. N. Tufte and P. W. Chapman, Phys. Rev. **155**, 796 (1967).
[20]R. Gerson and H. Jaffe, J. Phys. Chem. Solids **24**, 979 (1963).
[21]L. Wu, T. S. Wu, C. C. Wei, and H. C. Liu, J. Phys. C **16**, 2823 (1983).
[22]S. M. Sze and K. K. Ng, *Physics of Semiconductor Devices* (John Wiley & Sons, Hoboken, 2007).
[23]W. Walukiewicz, Physica B **302-303**, 123 (2001).
[24]S. B. Zhang, S.-H. Wei, and A. Zunger, J. Appl. Phys. **83**, 3192 (1998).
[25]A. Zunger, Appl. Phys. Lett. **83**, 57 (2003).
[26]J. Robertson and S. J. Clark, Phys. Rev. B **83**, 075205 (2011).
[27]A. D. Katnani and G. Margaritondo, Phys. Rev. B **28**, 1944 (1983).
[28]E. T. Yu, J. O. McCaldin, and T. C. McGill, Solid State Phys. **46**, 1 (1992).
[29]R. Schafranek, S. Payan, M. Maglione, and A. Klein, Phys. Rev. B **77**, 195310 (2008).
[30]F. Chen, R. Schafranek, W. Wu, and A. Klein, J. Phys. D: Appl. Phys. **42**, 215302 (2009).
[31]R. Schafranek, J. Schaffner, and A. Klein, J. Eur. Ceram. Soc. **30**, 187 (2009).
[32]F. Chen, R. Schafranek, S. Li, W. B. Wu, and A. Klein, J. Phys. D: Appl. Phys. **43**, 295301 (2010).
[33]F. Chen, R. Schafranek, A. Wachau, S. Zhukov, J. Glaum, T. Granzow, H. von Seggern, and A. Klein, J. Appl. Phys. **108**, 104106 (2010).
[34]S. Li, C. Ghinea, T. Bayer, M. Motzko, R. Schafranek, and A. Klein, J. Phys. Condens. Matter (to be published).
[35]D. Ensling, A. Thissen, Y. Gassenbauer, A. Klein, and W. Jaegermann, Adv. Engin. Mater. **7**, 945 (2005).
[36]R. L. Anderson, IBM J. Res. Dev. **4**, 283 (1960).
[37]J. Tersoff, Phys. Rev. B **30**, 4874 (1984).
[38]G. Margaritondo, Rep. Prog. Phys. **62**, 765 (1999).
[39]W. Ranke, Phys. Rev. B **27**, 7807 (1983).
[40]J. Goniakowski, F. Finocchi, and C. Noguera, Rep. Prog. Phys. **71**, 016501 (2008).
[41]A. Klein, C. Körber, A. Wachau, F. Säuberlich, Y. Gassenbauer, R. Schafranek, S. P. Harvey, and T. O. Mason, Thin Solid Films **518**, 1197 (2009).

[42] M. V. Hohmann, P. Ágoston, A. Wachau, T. J. M. Bayer, J. Brötz, K. Albe, and A. Klein, J. Phys. Condens. Matter (to be published).
[43] V. E. Henrich, G. Dresselhaus, and H. J. Zeiger, Phys. Rev. B **17**, 4908 (1978).
[44] R. Courths, Phys. Status Solidi B **100**, 135 (1980).
[45] B. Cord and R. Courths, Surf. Sci. **162**, 34 (1985).
[46] R. Schafranek and A. Klein, Solid State Ionics **177**, 1659 (2006).
[47] A. V. Dixit, N. R. Rajopadhye, and S. V. Bhoraskar, J. Mater. Sci. **21**, 2798 (1986).
[48] J. F. Scott, K. Watanabe, A. J. Hartmann, and R. N. Lamb, Ferroelectrics **225**, 83 (1999).
[49] S. Y. Li, A. Wachau, R. Schafranek, A. Klein, Y. L. Zheng, and R. Jakoby, J. Appl. Phys. **108**, 014113 (2010).
[50] Y. Gassenbauer, A. Wachau, and A. Klein, Phys. Chem. Chem. Phys. **11**, 3049 (2009).
[51] A. Klein, C. Körber, A. Wachau, F. Säuberlich, Y. Gassenbauer, S. P. Harvey, D. E. Proffit, and T. O. Mason, Materials **3**, 4892 (2010).
[52] S.-H. Wei and A. Zunger, Appl. Phys. Lett. **72**, 2011 (1998).
[53] T. Schulmeyer, R. Hunger, M. Lebedev, W. Jaegermann, A. Klein, R. Kniese, and M. Powalla, Thin Solid Films **480-481**, 110 (2005).
[54] J. E. Jaffe and A. Zunger, Phys. Rev. B **29**, 1882 (1984).
[55] Y. Ogo, H. Hiramatsu, K. Nomura, H. Yanagi, T. Kamiya, M. Hirano, and H. Hosono, Appl. Phys. Lett. **93**, 032113 (2008).
[56] L. Pintilie and M. Alexe, J. Appl. Phys. **98**, 124103 (2005).
[57] L. Pintilie, I. Vrejoiu, D. Hesse, G. LeRhun, and M. Alexe, Phys. Rev. B **75**, 104103 (2007).
[58] A. Zunger, Phys. Rev. Lett. **54**, 849 (1985).
[59] J. M. Langer, C. Delerue, M. Lannoo, and H. Heinrich, Phys. Rev. B **38**, 7723 (1988).
[60] M. Turcu, I. M. Kötschau, and U. Rau, J. Appl. Phys. **91**, 1391 (2002).
[61] J. Robertson, K. Xiong, and S. J. Clark, Thin Solid Films **496**, 1 (2006).
[62] O. Saburi, J. Phys. Soc. Jpn. **14**, 1159 (1959).
[63] P. Erhart and K. Albe, J. Appl. Phys. **102**, 084111 (2007).
[64] J. Son, P. Moetakef, B. Jalan, O. Bierwagen, N. J. Wright, R. Engel-Herbert, and S. Stemmer, Nature Mater. **9**, 482 (2010).
[65] S. Steinsvik, R. Bugge, J. Gjønnes, J. Taftø, and T. Norby, J. Phys. Chem. Solids **58**, 969 (1997).
[66] M. V. Raymond and D. M. Smyth, Integrated Ferroelectrics **4**, 145 (1994).
[67] Y. Gassenbauer, R. Schafranek, A. Klein, S. Zafeiratos, M. Hävecker, A. Knop-Gericke, and R. Schlögl, Phys. Rev. B **73**, 245312 (2006).